ICAS-88-4.6R1

Boundary Conditions for Viscous Incompressible Two Dimensional Flows

A. Dagan and R. Arieli
Rafael - Haifa, Israel

Abstract

A preliminary study of the numerical solution of the incompressible Navier-Stokes equations in their vorticity/stream function formulation is presented. Two different numerical techniques are compared, a pseudo-spectral method and an ADI scheme, in the solution of viscous flow around circular and elliptical cylinders. The numerical solution using the ADI scheme is reliable, robust and accurate for both transient and periodic "steady state" conditions. The pseudo-spectral algorithm is as accurate as the ADI solution for transient conditions, but is considerably slower.

1. Introduction

Slender body theory is widely used in aerodynamic analysis and design. With a well defined vortex system, many moderate to high angle of attack flows are successfully modeled by the classical superposition of an attached flow and a vortical detached one [1]. The technique requires knowledge of the sectional drag coefficient in the cross flow direction. Since this type of data is available predominantly from experimental investigations, it is obviously restricted to a limited number of cross sections. Indeed, the method is frequently used for conventional configurations, but only a few attempts have been made to extent it for noncircular bodies [2].

With the growing interest in the aerodynamic characteristics of smooth, noncircular bodies, a pressing need has been felt to develop a basis for simple engineering design model suitable for slender wings and bodies at various speeds and angles of attack, providing the flow is quasi steady.

It is anticipated that accurate numerical calculations of the two-dimensional drag coefficient for arbitrary cross sections will further extent this existing, well proven aerodynamic technique. However, in order to study the feasibility of the proposed approach, a preliminary evaluation of existing 2D numerical methods for the solution of viscous flow is required.

In recent years, a wide range of numerical techniques aiming at the solution of viscous flows problems, have been proposed [3][4][5]. Many of them successfully simulate real flow effects for two-dimensional as well as for three-dimensional cases. However, viscous flow simulations are still under continuous development and generally they still require extensive computing time and resources. In the present study two numerical algorithms are compared, the one is a common finite differences approach based on an ADI technique, and the other uses a pseudo-spectral method.

Spectral techniques are very efficient in solving Poisson's equation for a prescribed level of accuracy [6]. The main advantage of this technique is its exponential rate of convergence. However, in order to take advantage on the spectral technique using Fourier representation, the problem under consideration must be periodic at least in one direction. For the case of a two dimensional flow, this is not a severe restriction, providing the flow equations are reformulated in a polar type coordinate system. An additional important feature of this method is the absence of significant artificial viscosity.

On the other hand, finite differences algorithms like the ADI, are robust, and flexible in handling boundary conditions [7]. This type of algorithms is well established and widely used in many CFD fields, its behavior is well understood and the effort associated with its programming is modest.

In the remaining of the paper, the mathematical formulation is presented in chapter 2, the numerical implementation in chapter 3, followed by some results and discussion.

2. Governing Equations

In order to gain a better insight and understanding of the acting mechanisms, the authors believe that the vorticity/stream function formulation is superior to that using primitive variables. To the extend of our understanding, the vorticity plays the major role in all possible scenarios of lift generation. Therefore it is only natural that the numerical simulation ought to correctly describe both the generation and the convection of vorticity throughout the flow field in order to offer a meaningful lift prediction.

For simplicity, in the present study incompressible flows

are examined. This simplification reduces the amount of numerical work without a significant loss in generality, since compressibility effects are easily accounted for subcritical flows, while for supercritical cases an additional logic must be included to enter correctly in the appropriate branch.

The vorticity stream function formulation for this type of flows is:

$$\frac{\partial \omega}{\partial t} + u\frac{\partial \omega}{\partial x} + v\frac{\partial \omega}{\partial y} = \frac{1}{Re}\nabla^2\omega \qquad (1)$$
$$\nabla^2\psi = \omega$$

where ω is the vorticity, ψ is the stream function, and the Reynolds number $Re = U_\infty l/\nu$ is based on the free stream velocity U_∞ and the length scale l which in the present study denotes the sectional width.

The right hand side describes the diffusion of the vorticity, while the left hand side represent the convection of vorticity. It is worth mentioning here that the stretching of the vortex tube, which is an important mechanism in the vorticity equation is unique to the 3-D formulation, and is completely removed in the 2-D approximation.

The initial conditions for the general case of flow over a solid body is characterized by a generation of zero thickness vortex sheet that warp the solid surface. Mathematically, this vortex sheet is represented at its initial time stage by a Dirac function. At any latter stage, that involves diffusion of the vortex sheet into the flow field, where the convection terms become the main mechanism in the vorticity transport equation. Thus, the proper description of the vorticity at the initial time stage is a major numerical difficulties encountered, while solving these equations.

The boundary conditions required for the numerical simulation of a viscous two dimensional flow, are the no slip condition along the solid surface and the far field conditions along the outer boundary. While using vorticity and stream function as the dependent variables, another set of conditions must be supplied. The first difficulty originated from the vorticity/stream function formulation is the solid surface boundary condition. In the present formulation an implicit condition is required along the surface, thus coupling the two equations. The far field boundary conditions, in terms of stream function and vorticity, are well defined if the boundary lies at infinity. However, for a finite size computational domain, a outflow boundary condition has to be imposed on both variables. As long as the entire vorticity is confined into the computational domain, zero vorticity and a multipole behavior of the stream function [8] are adequate conditions. However, the use of these conditions is limited by time. When the vorticity is convected through the computational domain, it is assumed that the outer boundary is at a sufficient distance to allow negligibly small diffusion terms. Thus, the conditions imposed on the vorticity are those of an inviscid flow [3]. The boundary conditions for the stream function have been modified similarly to those of the vorticity.

3. Numerical Approximation

Pseudo-Spectral Method

Using a conformal mapping to transform any section under consideration from the physical domain defined by a set of cartesian coordinates x and y, onto a computational domain $x + iy = f(\xi)$, where ξ is the computational plane defined by $\xi = re^{i\theta}$. The flow is always periodic in the circumferential direction therefore the vorticity and stream function can be written;

$$B = \sum_{n=-\infty}^{\infty} B_n e^{in\theta}$$

$$\omega = \sum_{n=-\infty}^{\infty} \omega_n e^{in\theta}$$

$$\psi = \sum_{n=-\infty}^{\infty} \psi_n e^{in\theta}$$

where $B = J_0\omega$, and $J_0 = f_\xi f_{\bar{\xi}}^*$ is the Jacobian of the transformation. B_n, ω_n and ψ_n are the Fourier coefficients respectively. By using this type of transformation, the grid generated in the computational domain is orthogonal. Probably, the main advantage of an orthogonal mesh is the simplification of all the terms in the equation, by eliminating all existing mixed derivatives. Upon substitution the following equations are obtained;

$$B^\kappa_{n,j} - B^{\kappa-1}_{n,j} + \Delta t D_{n,j} = \frac{\Delta t}{Reh^2}\{\frac{1}{r_j}\delta_r(r_j\delta_r) - \frac{n^2}{r_j^2}\}\omega^\kappa_{n,j}$$

$$\{\frac{1}{r_j}\delta_r(r_j\delta_r) - \frac{n^2}{r_j^2}\}\psi^\kappa_{n,j} = B^\kappa_{n,j} \qquad (2)$$

where $D_{n,j}$ is the inverse transformation of the convection terms for each Fourier mode. The number of computer operation required to compute the nonlinear term is proportional to $O(NMlogM)$. Where N denotes the number of grid points in the radial direction, however M is the number of spectral modes which is smaller then the number of grid points in the θ direction.

For each mode n, the linear part of equation (2) is written in a tri-diagonal form, yielding the vorticity distribution and the stream function at the $\kappa + 1$ time level.

$$\begin{Bmatrix} a_j^{(3)}, 0 \\ 0 \quad , b_j^{(3)} \end{Bmatrix} \begin{Bmatrix} B_{n,j-1} \\ \psi_{n,j-1} \end{Bmatrix} + \begin{Bmatrix} a_j^{(2)}, 0 \\ -1, b_j^{(3)} \end{Bmatrix} \begin{Bmatrix} B_{n,j} \\ \psi_{n,j} \end{Bmatrix} +$$

$$+ \begin{Bmatrix} a_j^{(1)}, 0 \\ 0 \quad , b_j^{(1)} \end{Bmatrix} \begin{Bmatrix} B_{n,j+1} \\ \psi_{n,j+1} \end{Bmatrix} = \begin{Bmatrix} F_j \\ q_j \end{Bmatrix}$$

where the terms a_j are the coefficients of equation (2). The vorticity, velocities and their first derivative obtained at $\kappa+1$, are than transformed to the physical domain with the use of a F.F.T algorithm. By using the inverse transformation of the F.F.T. Then all the $D_{n,j}$'s are obtained at time level $\kappa+1$.

The kinematic boundary condition, and the no-slip condition have been expressed accordingly to Lugt [3] as:

$$\omega_{n,1} = \frac{8\psi_{2,n} - \psi_{3,n}}{2h^2} + O(h^2)$$

$$\psi_{1,n} = 0$$

As long as the vorticity is confined in the computational domain, the downstream boundary condition is easily reduced to the multipole behavior of the stream function i.e:

$$\frac{\partial \psi_n}{\partial r} + \frac{n}{r}\psi_n = -iU_\infty e^{-i\alpha}\delta_{n,1} \qquad n = 1,2,3...$$

where $\delta_{n,k} = 1$ if $n = k$, and $\delta_{n,k} = 0$ if $n \neq k$. For $n = 0$ the asymptotical behavior of the ψ_0 is reduced to the circulation theorem i.e;

$$\psi_0 = \frac{\Gamma}{2\pi} lnr$$

where

$$\Gamma = \int\int_A \omega dA$$

Since the vorticity is convected by the local velocity, and in the same time diffused, the assumption that $\omega_{n,N} = 0$, is acceptable as long as the vorticity is confined in the computational domain.

ADI Method

Although the spectral method seems to be competitive with the traditional finite difference method, there are still problems that must be solved. One of them is the severe restriction on the size of the time step, resulting from the CFL condition. Thus, equation (1) is reformulated with the use of an ADI method [9] in order to reconstruct the proper downstream numerical boundary condition for a finite computational domain.

Considered $\psi^{\kappa+1} = \psi^\kappa + \psi_1$, and $\omega^{\kappa+1} = \omega^\kappa + \omega_1$, where all quantities with subscript 1 denotes the correction at the time level $\kappa+1$. The vorticity equation and the stream function equation are rewritten in a non-conservative form, in the ξ plane as;

$$[I + \Delta tA][I + \Delta tC]X = f$$

where

$$A = \begin{Bmatrix} \frac{v_r^\kappa}{J_0}\delta_j - \frac{1}{ReJ_0 r_j}\delta_j(r_j\delta_j), & \frac{1}{rJ_0}\frac{\partial \omega^\kappa}{\partial \theta}\delta_j \\ \frac{J_0}{\alpha} & , -\frac{1}{\alpha r_j}\delta_j(r_j\delta_j) \end{Bmatrix}$$

$$C = \begin{Bmatrix} \frac{v_\theta^\kappa}{rJ_0}\delta_i - \frac{1}{ReJ_0 r_j^2}\delta_i^2, & \frac{1}{rJ_0}\frac{\partial \omega^\kappa}{\partial r}\delta_i \\ 0 & , -\frac{1}{\alpha r_j^2}\delta_i^2 \end{Bmatrix}$$

and

$$X = \begin{Bmatrix} \omega_1 \\ \psi_1 \end{Bmatrix}$$

where f is finite difference approximation of Eq. (1) at time level κ. r_j is the radial possition, v_r and v_θ are the radial and circumferential velocity components respectively.

A pseudo time step ($\alpha\Delta t\partial_t\psi$) is added to the stream function equation in order to make it of a parabolic type, which is necessary for the ADI formulation. The parameter α is chosen arbitrarily (value 0f 1 has been used). This scheme turns to be numerically more stable compared to the pseudo-spectral algorithm.

The downstream boundary condition can be approximated as:

$$\frac{\partial \omega}{\partial t} + U\frac{\partial \omega}{\partial x} = 0$$

which essentially is the Oseen approximation. Upon substitution

$$\nabla^2\left\{\frac{\partial \psi}{\partial t} + U\frac{\partial \psi}{\partial x}\right\} = 0$$

which yields

$$\frac{\partial \psi}{\partial t} + U\frac{\partial \psi}{\partial x} = \sum_{n=0}^{\infty}\frac{a_n}{r^n}e^{in\theta}$$

However, in this study the right hand side of the obtained downflow boundary condition has been set to zero. Unfortunately we do not have a solid justification for neglecting this term, except that the operator $\partial_t + U\partial_x$ may permit the stream function to convect in the same sense as the vorticity convection i.e;

$$\{\frac{\partial}{\partial t} + U\frac{\partial}{\partial x}\}\{\psi, \omega\} \qquad (3)$$

4. Results and Discussion

Several numerical test cases have been conducted in order to verify the capabilities of the two methods. The first case is a flow over a circular cylinder, at low Reynolds number flow conditions (Re = 5 to 20). Low Reynolds number is used to prevent vorticity from leaving the computational domain. The results of the pseudo spectral calculation are illustrated in figures 1 and 2, these results are qualitatively in good agreement with the experimental results of Van Dyke [10]. The pseudo-spectral solution converges fast, only 8 spectral modes are required to get to the single precision machine zero.

The stream line pattern for a flow past an elliptic cylinder is shown in Fig. 3 and 4 , where the Reynolds number for both cases is 100, while the latter is at 45^0 incidence.

The vorticity contours obtained using the ADI method with the downstream boundary conditions (Eq. 3) are illustrated in figures 5 through 8. It is easy to verify that the boundary conditions do not cause any kind of reflection problem. The wiggles appearing in Fig. 7, are the result of insufficient resolution in the circumferential direction along the computational boundary. Fig. 8 shows the computed results of the vorticity contours at a time when a new vortex core is generated near the trailing edge while the previous vortex has been convected far downstream (about one body widths away). This sequence of flow pattern repeats itself until a complete stage of Von Karman vortex-street is generated.

Figures 9 through 11 show the instantaneous stream lines pattern of the same flow field. However it can be noticed that the approximated downstream boundary condition for the stream function works well. The boundary condition (Eq. 3) has been further simplified by replacing the x direction of the original b.c. by the r direction, thus yielding in the final approximation:

$$\{\psi,\omega\}^{\kappa+1} = \{\psi,\omega\}^{\kappa}(r - U\triangle t)$$

This downstream boundary condition generate a small slope discontinuity in the stream lines in the vicinity of the computational boundary, but this has only a local influence and does not affect the solution at large (Fig 10,11).

The comparison between the measured [11] and the computed drag coefficient over a flat plate is shown in Fig. 12 (Re=100).

It can be observed that due to the symmetric case that has been employed, no effect from the Von Karman street vortex is introduced in the results. Thus the asymmetric disturbance resulting from the numerical scheme, is too small to generate the Von Karman street vorticies.

To conclude, two numerical algorithms have been tested and compare for the case of incompressible flow about infinite circular and elliptical cylinders. The elliptical cross section has been tested in symmetric and asymmetric flow conditions. All numerical experiments have been conducted on an orthogonal mesh of 60 x 100 grid points in the radial and circumferential directions respectively. No symmetry has been imposed on the solutions, still only in the elliptical cross section at incidence the Von-Karman vortex street flow pattern has ban reached. When the methods are compared on an accuracy basis, the two are very similar. However, they are extremely apart when their efficiency is verified. For a transient type solution, after a non dimensional time of 5 (the time required to a particle to travel five body widths) the spectral method solution takes about 60 min on a DEC-8700 machine, while the ADI solution requires about 5 min. This enormous difference in computing effort is directly related to the very severe restriction on the size of the time step due to the CFL condition. At the present stage in time the cost of the pseudo-spectral solution is prohibitively high for all practical purposes. On the other hand, the ADI method appear suitable to be part on a prediction code.

5. References

1 Hemsch, M.J. and Nilsen, J.N.; "The Equivalent Angle-of-Attack Method for Estimating the Nonlinear Aerodynamic Characteristics of Missile Wings and Control Surfaces", AIAA-82-1338 paper, August, 1982.

2 Hemsch, M.J.; "Similarity for High Angle-of-Attack Subsonic/Transonic Slender-Body Aerodynamics", AIAA-88-0216 paper, January, 1988.

3 Lugt, H.J., Haussling, H.J.; "Laminar Flow Past an Abruptly Accelerated Elliptic Cylinder at 45^0 Incidence", J. of Fluid Mech. Vol. 65, Part 4, pp.711-734, 1974.

4 Ta Phuoc Loc; "Numerical Analysis of Unsteady Secondary Vorticies Generated by an Impulsively Started Circular Cylinder", J. Fluid Mech, Vol. 100, Part 1, pp. 111-128, 1980.

5 Shida, Y., Kuwahara, K. and Takami, H.; "Computation of Dynamic Stall of NACA-0012 Airfoil", AIAA J. Vol. 25, No. 3, 1987.

6 Orszag, S. and Patera, A.T.; "Secondary Instability of Wall Bounded Shear Flow", J, Fluid Mechanics, Vol. 128, 1983. pp. 347-385.

7 Roache, P.J.; "Computational Fluid Dynamics", Hermosa Pub., Albuquerque, N.M. 1972.

8 Fasel, H.; "Investigation of the stability of boundary layers by finite difference model of N-S equation",J. Fluid Mech., Vol. 78, Part 2,1976, pp. 355-383

9 Steger, J.L. and Van Dalsem, W.R.; "Developments in the Simulation of Separated Flows using Finite Difference Methods", Proceedings of the 3ed Symposium on Numerical and Physical Aspects of Aerodynamic Flow, Cal. State Universitu, Long Beach, California, January 21-24, 1985.

10 Van Dyke, M.; "An Album of Fluid Motion", The Parabolic Press, Stanford, Calif., 1982.

11 Hoerner, S.F.;"Fluid Dynamic Drag", Published by the author, 1965.

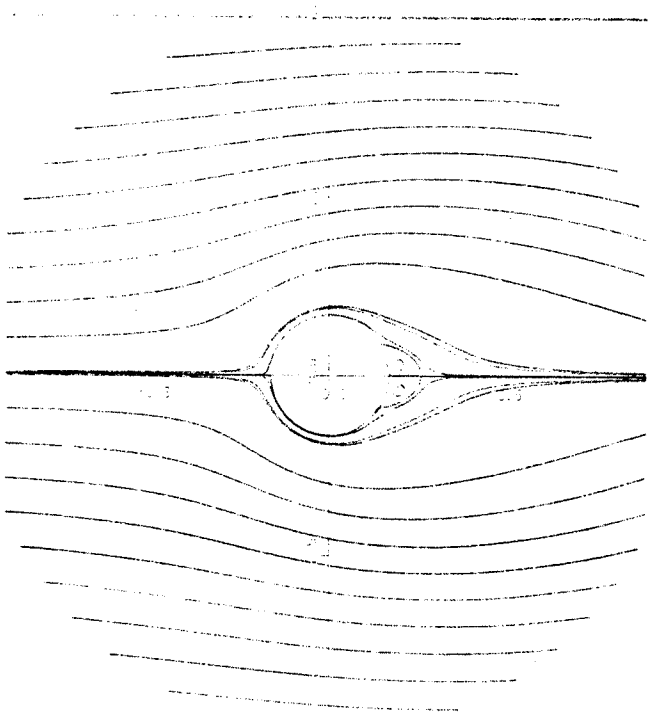

Fig. 1 Pseudo Spectral solution of laminar flow past a circular cylinder Re=6.5

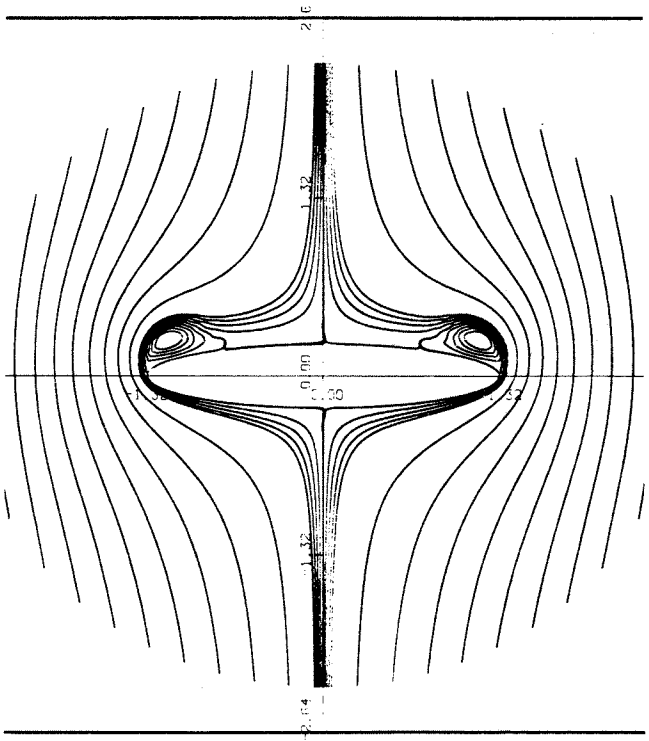

Fig. 3 Pseudo Spectral solution of laminar flow past an elliptical cylinder Re=6.5.

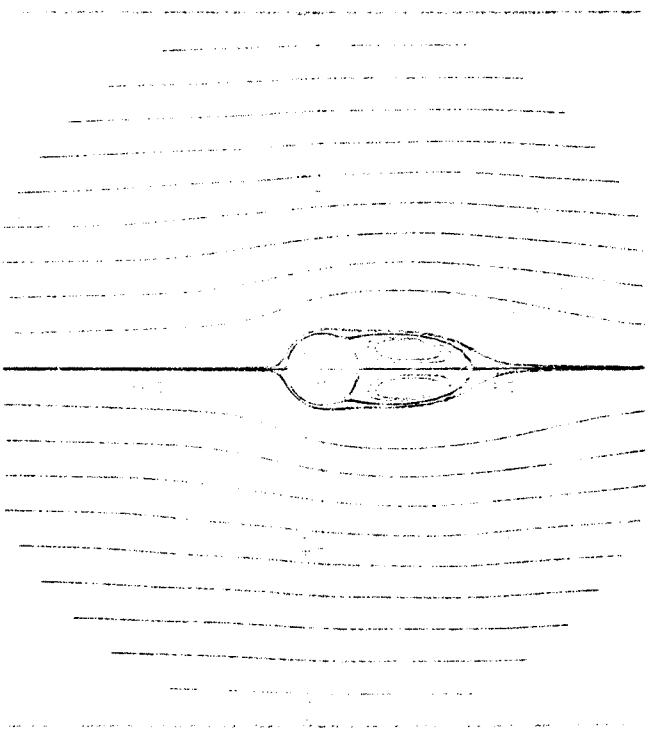

Fig. 2 Pseudo Spectral solution of laminar flow past a circular cylinder Re=20.

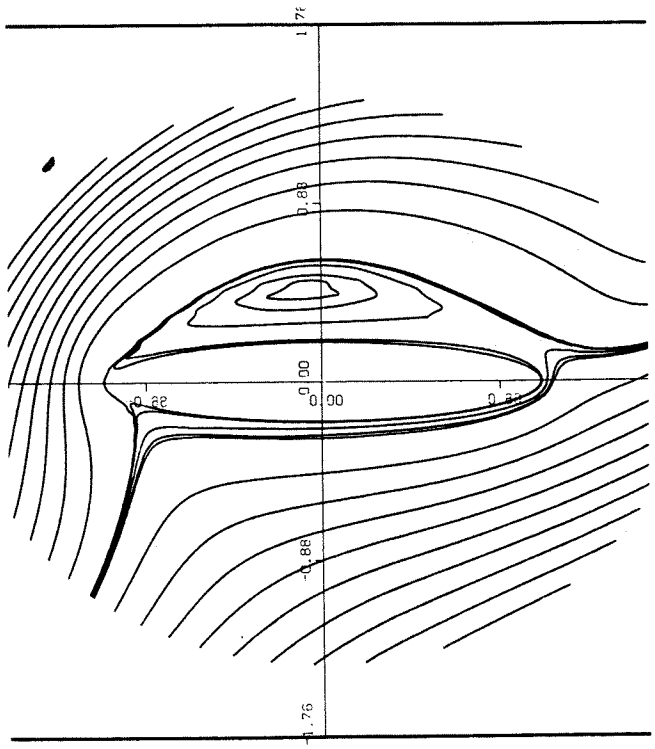

Fig. 4 Pseudo Spectral solution of laminar flow past an elliptical cylinder Re=20.

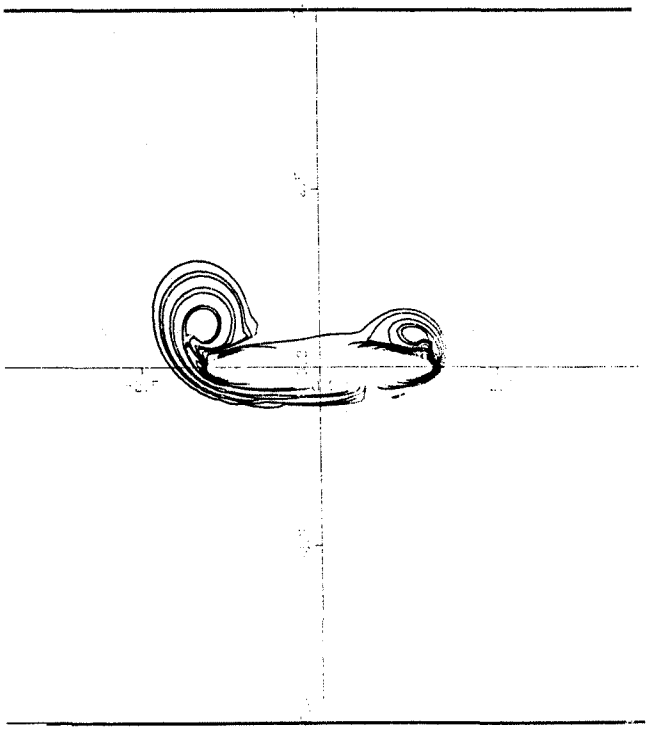

Fig. 5 Vorticity Contours for Laminar flow past an elliptical cylinder at $T = .6$ and Re=100 (ADI).

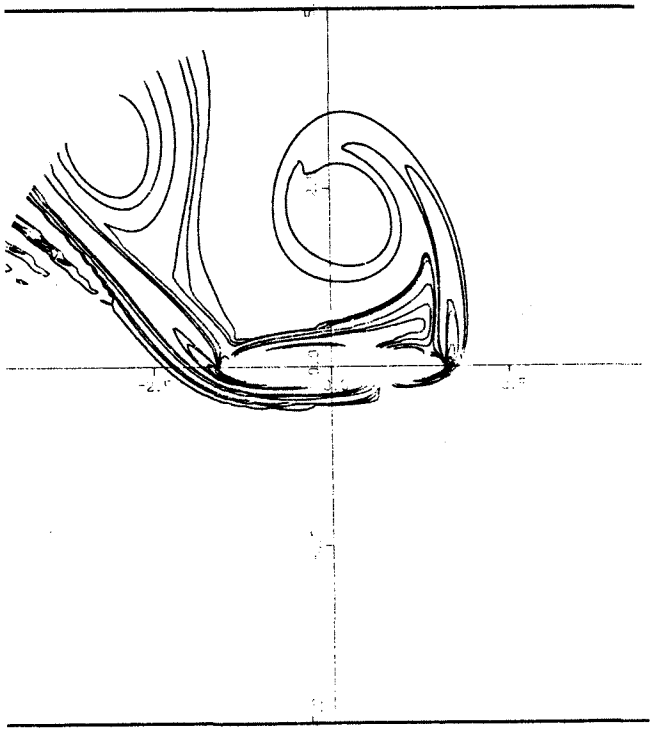

Fig. 7 Vorticity Contours for Laminar flow past an elliptical cylinder at $T = 1.8$ and Re=100 (ADI).

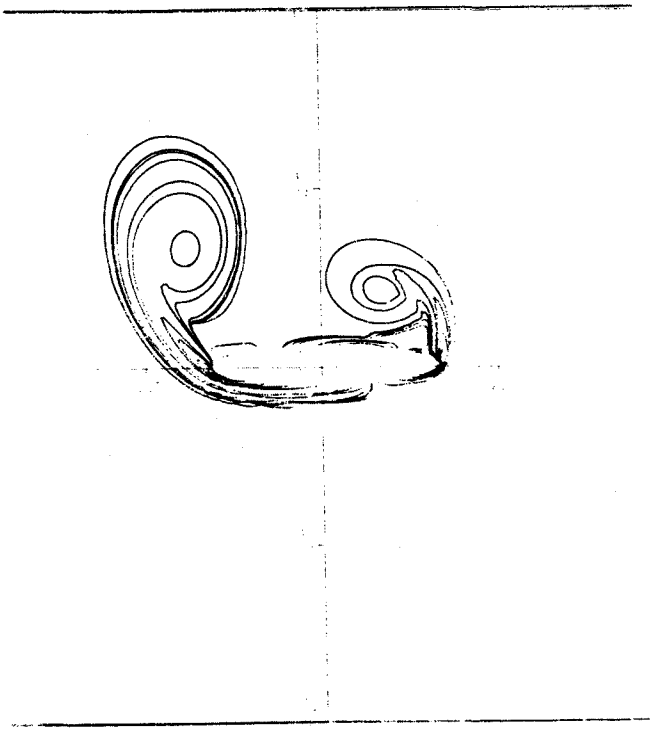

Fig. 6 Vorticity Contours for Laminar flow past an elliptical cylinder at $T = 1.2$ and Re=100 (ADI).

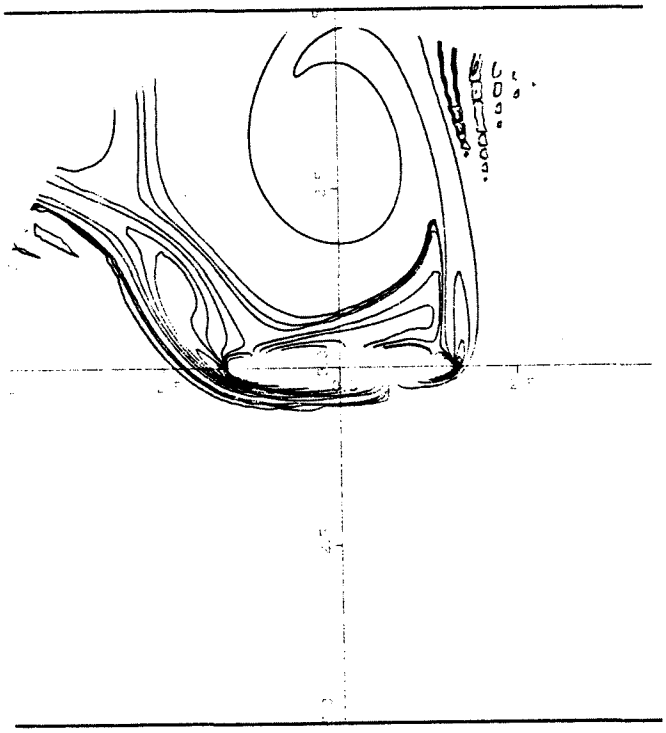

Fig. 8 Vorticity Contours for Laminar flow past an elliptical cylinder $T = 2.4$ and Re=100 (ADI).

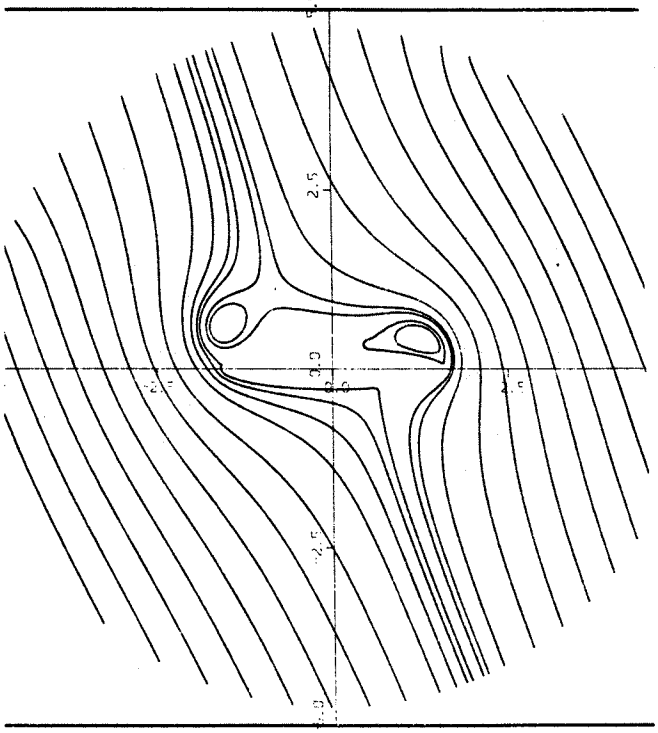

Fig. 9 Stream function Contours for Laminar flow past an elliptical cylinder $T = .6$ and Re=100 (ADI).

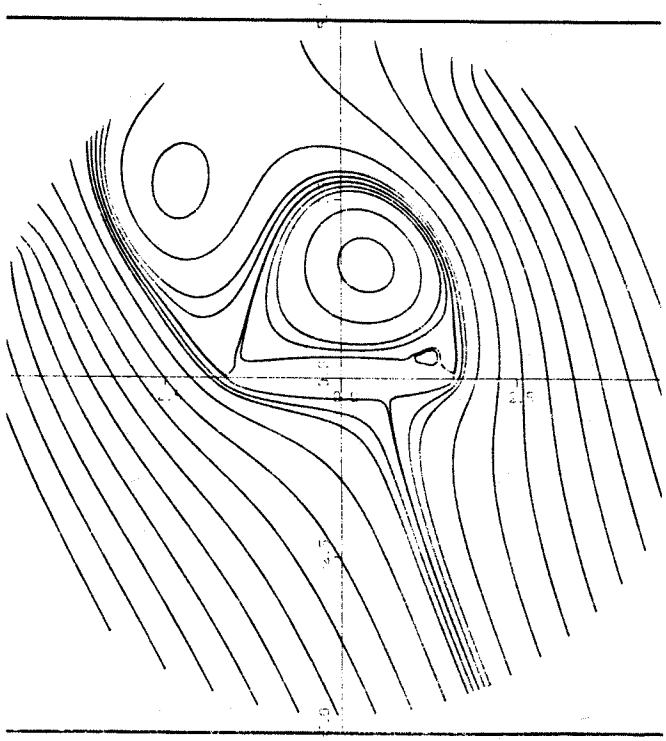

Fig. 10 Stream function Contours for Laminar flow past an elliptical cylinder $T = 1.2$ and Re=100 (ADI).

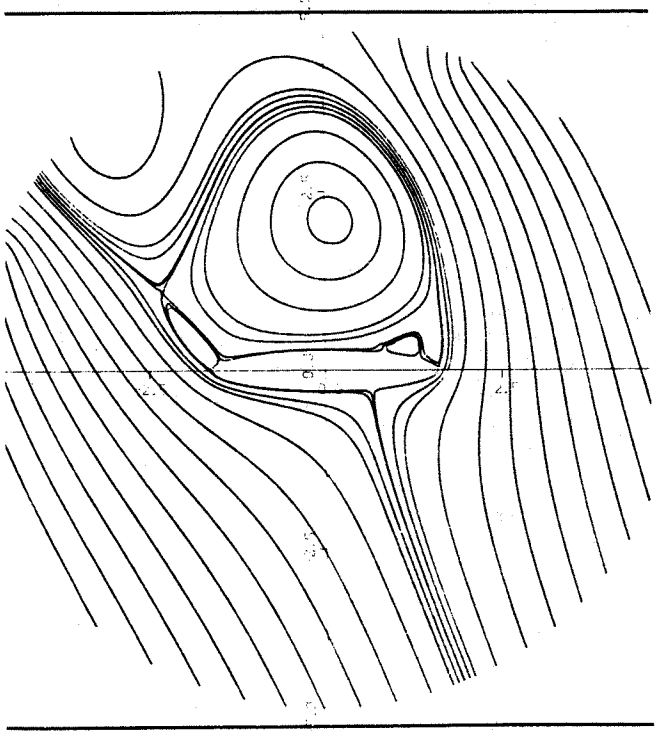

Fig. 11 Stream function Contours for Laminar flow past an elliptical cylinder $T = 1.8$ and Re=100 (ADI).

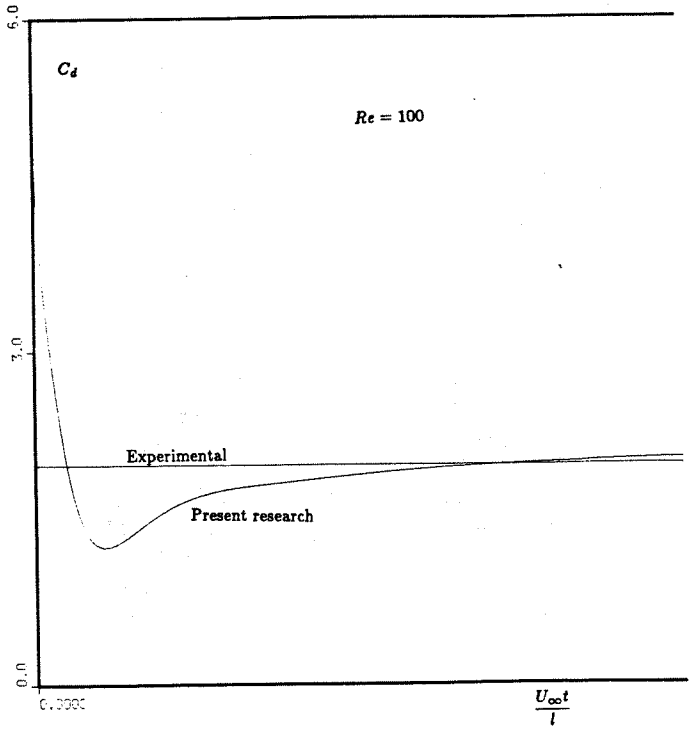

Fig. 12 Drag coefficient over a flat plate at RE=100 (ADI).